

# TEST-ANALYSIS CORRELATION AND FINITE ELEMENT MODEL UPDATING FOR NONLINEAR, TRANSIENT DYNAMICS

François M. Hemez<sup>1</sup> and Scott W. Doebling<sup>2</sup>

Engineering Sciences & Applications, ESA-EA, M/S P946  
Los Alamos National Laboratory, Los Alamos, NM 87545

## ABSTRACT

This research aims at formulating criteria for measuring the correlation between test data and finite element results for nonlinear, transient dynamics. After reviewing the linear case and illustrating the limitations of modal-based updating when it is applied to nonlinear experimental data, simple time-domain, test-analysis correlation metrics are proposed. Two implementations are compared: the conventional least-squares technique and the Principal Component Decomposition that correlates subspaces rather than individual time-domain responses. Illustrations and discussions are provided using the LANL 8-DOF system, an experimental testbed for validating nonlinear data correlation and model updating techniques.

## NOMENCLATURE

The recommended "Standard Notation for Modal Testing & Analysis" proposed in Reference [1] is used throughout this paper.

## 1. INTRODUCTION

The recondite nature of nonlinearity has made development of correct analytical models of nonlinear systems a difficult task. Although analytic methods and numerical tools are available for modeling specific types of nonlinearity, a systematic investigation of the formulation and resolution of inverse problems for nonlinear dynamics has never, to the best of our knowledge, been addressed in the literature. This work summarizes such an investigation and illustrates the issues of nonlinear

finite element (FE) updating with a simple yet realistic testbed.

Handling nonlinear models is generally something analysts prefer to avoid because it too often stretches to their limits our mathematical tools and points to our lack of understanding of the physics of structural dynamics. Nevertheless, improving performances requires to account for the true, nonlinear nature of structural systems and, therefore, it can be predicted that the field of conventional modal analysis will increasingly involve nonlinearity as structural designs are increasingly being optimized.

When modal analysis is performed, structural systems are usually tested and analyzed under the assumption that the behavior remains linear in the frequency range of interest. This fundamental assumption makes it possible to interpret data in the frequency domain because signals measured or simulated through finite element analysis can generally be found periodic. On the other hand, analyzing nonlinear systems based on Fourier superposition or other modal transforms would theoretically require the addition of higher-dimensional kernels, the definition of which depends on the type of nonlinearity encountered [2]. Another drawback is that most transformations, such as Fourier transforms, wavelets or Singular Value Decomposition (SVD), are essentially linear tools: there is a theoretical limitation at analyzing nonlinear data with linear techniques. This motivates our choice of attempting to instrument and correlate FE models in the time domain, even though this choice adds difficulties that the frequency-domain approach allows to bypass.

This research aims at formulating criteria for measuring the correlation between test data and finite

---

<sup>1</sup> Technical Staff Member, ESA-Engineering Analysis Group (hemez@lanl.gov), Member SEM.

<sup>2</sup> Senior Technical Staff Member, ESA-Engineering Analysis Group (doebing@lanl.gov), Member SEM.

*Published at the 17th International Modal Analysis Conference, February 8-11, 1999, Kissimmee, Florida.*

© Copyright 1998, 1999 by F.M. Hemez, S.W. Doebling and Los Alamos National Laboratory, Los Alamos, NM.

**Approved For Public Release/Unlimited Distribution, LAUR-98-4573.**

element results for nonlinear, transient dynamics. We place a particular emphasis on developing a methodology that can handle any type and source of nonlinearity, therefore, requiring both parametric and non-parametric model updating. Typical examples of nonlinearities we are interested in include material nonlinearity, friction, impact and contact at the interface between two components. These are typical of nonlinearity sources dealt with in the automotive and aerospace industries. The study of geometrical nonlinearity, on the other hand, is extensively covered in the literature: accurate models that handle, for example, large displacements and/or large deformations can be obtained using the adequate variational principles and FE discretizations [3].

In this paper, the effectiveness of a rather classical time-domain, least-squares comparison between measured and simulated responses is assessed using two implementations. The first one correlates directly the measured and simulated signals while the second one focuses more specifically on correlating the subspaces to which these signals belong. Demonstration examples using simulated and real test data illustrate ideas proposed and offer a discussion of issues regarding the implementation of these techniques.

## 2. EXPERIMENTAL TESTBED

The LANL 8-DOF (which stands for Los Alamos National Laboratory eight degrees of freedom) testbed consists of eight masses connected by linear springs. The masses are free to slide along a center rod that provides support for the whole system. Boundary conditions are unrestrained. Figure 1 shows the experimental testbed. It is instrumented with eight accelerometers and excitation is provided using either a hammer or a shaker. The first degree of freedom where the excitation is applied provides a driving point measurement for identification purposes. The advantage of the LANL 8-DOF testbed is that it can be modeled fairly accurately using a linear, mass-spring system. Nevertheless, the correlation of FE simulations with test data illustrates the limitation of a linear modeling approach, as seen in Section 4.

Modal tests are performed on the nominal system and on a damaged version where the stiffness of the fifth spring is reduced by 14%. A contact mechanism can also be added between masses 5 and 6 to induce a source of contact/impact between these two masses. The system is then tested under various excitation levels to assess the

degree of nonlinearity. Time-domain responses are measured at each one of the 8 masses and modal parameters are identified using a classical frequency-domain curve fitting algorithm.

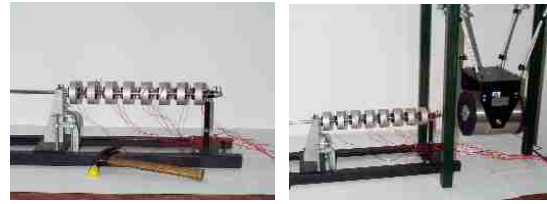


Figure 1: LANL 8-DOF Testbed.

Table 1 compares the first five modes identified with the nominal and damaged systems, both in the linear configuration (the contact/impact mechanism is removed). Hammer excitations and data averaging are used for these series of tests. Large damping ratios can be observed. It suggests that the sliding mechanism and the friction it generates play an important role in the dynamics measured. These high damping ratios are produced artificially when the identification algorithm attempts to best-fit the measured response using (implicitly) a proportional damping model. Also, the reduction of stiffness translates, as expected, into a reduction of modal frequencies. However, it can be stated from frequencies in Table 1 and a visual comparison of mode shapes that this damage scenario has little overall effect on the response of the LANL 8-DOF system.

Table 1. Identified Modal Parameters For the Nominal and Damaged Systems.

Nominal Frequency	Modal Damping	Damaged Frequency	Modal Damping
22.6 Hz	8.5%	22.3 Hz	13.6%
44.5 Hz	4.3%	43.9 Hz	5.0%
65.9 Hz	3.3%	64.8 Hz	3.5%
86.6 Hz	5.0%	85.9 Hz	5.9%
99.4 Hz	2.6%	99.7 Hz	3.6%

Next, test-analysis correlation (TAC) results are shown in Table 2 between the identified modal parameters of the damaged system and results obtained with the nominal (undamaged) FE model. The modal assurance criterion (MAC) illustrates the excellent agreement between test and model vectors since most values are above 98%, despite the unmodeled stiffness reduction and the effect of friction. Although it clearly shows a systematic error (the first three modes are very well correlated but exhibit a systematic 2.4% frequency error in

average), the linear FE model is believed to be a good starting point for the optimization.

**Table 2. TAC Before FE Model Updating (Damaged System Vs. Nominal FE Model).**

Identified Frequency	FE Model Frequency	Frequency Error	MAC
22.3 Hz	21.8 Hz	-2.3%	99.7%
43.9 Hz	43.0 Hz	-2.0%	99.4%
64.8 Hz	63.0 Hz	-2.8%	99.4%
85.9 Hz	80.8 Hz	-6.0%	93.2%
99.7 Hz	95.6 Hz	-4.1%	98.5%

### 3. TAC FOR LINEAR SYSTEMS

One method of obtaining a correct representation is to create a finite element model of a system and correlate this model with measurement data taken from the system itself or some of its components. Applied essentially to linear systems, this approach has been found quite effective when modal data are used in the correlation process. In this case, the equation of motion can be written as

$$[M(p)]\{a(t)\} + [K(p)]\{u(t)\} = \{F_e(t)\} \quad (1)$$

which spells the equilibrium between inertia forces, internal (linear) forces and applied loading. In equation (1), the mass and stiffness matrices depend on design variables  $\{p\}$  which express the parametric nature of FE representations. We will see in the following that model updating is the procedure by which these variables  $\{p\}$  are optimized to minimize the distance between test data and FE simulations.

Since the dynamics are linear, the equilibrium (1) can be transformed in the frequency domain using a convolution operator (such as Laplace or Fourier transform). The resulting equation relates the input and output frequency response functions (FRF) of the system at any given sampling frequency  $\lambda$  as

$$([K(p)] - \lambda [M(p)]) \{u(\lambda)\} = \{F_e(\lambda)\} \quad (2)$$

Resonant frequencies  $\lambda$  and mode shapes  $\{\phi\}$  are extracted from the homogeneous version of equation (2). With orthogonality conditions added to equation (3) below, the mode shapes provide a basis for the subspace to which the response  $\{u(\lambda)\}$  belongs.

$$([K(p)] - \lambda [M(p)]) \{\phi\} = 0 \quad (3)$$

Experimentally, the system's modal parameters are identified from measured FRFs or directly from time-domain data using identification algorithms, a review of which can be found in Reference [4]. Hence, equations (1-3) emphasize the relationships between FE matrices and quantities measured or identified during modal tests. They form the basis of any TAC procedure: clearly, the system's correct representation is obtained when these equations are verified as measured quantities replace the FE outputs  $\{a(t)\}$ ,  $\{u(t)\}$ ,  $\{u(s)\}$  or  $(\lambda; \{\phi\})$  in equations (1-3).

Note that this formalism extends without difficulty to damped structural systems. In this case, modal parameters are complex quantities and the comparison between their real and imaginary parts provides information regarding the type of damping. The main difference between non-proportionally and proportionally damped systems is basically that the real and imaginary parts of mode shape vectors are not parallel in the former case. Note also that experimental procedures are available for dealing with damped systems. While most techniques apply to proportional damping only, some recent developments have proven efficient for reconstructing full-order, non-diagonal modal damping matrices [5].

#### 3.1 TAC & Linear FE Model Updating

Typical examples of TAC metrics that have been applied successfully to linear yet relatively sophisticated systems include minimum distance between identified and simulated frequencies, mode shapes [6] or frequency response functions [7], as well as the minimization of modal residues [8-9], the definition of which is summarized below. Obviously, the equation of vibration (3) is violated when FE modal parameters are replaced with test data as long as the parametric representation is erroneous. This inequality can be used for defining modal residue vectors  $\{Rf(p, \lambda)\}$  that account for the out-of-balance forces in the model as

$$[K(p)] \{\phi\} = \lambda [M(p)] \{\phi\} + \{Rf(p, \lambda)\} \quad (4)$$

Vectors  $\{Rf(p, \lambda)\}$  exhibit the largest entries at degrees of freedom (DOF) where the equilibrium is violated the most. This can be used as the basis for: 1) Identifying the source of modeling error; and 2) Updating the model by minimizing a norm of vectors  $\{Rf(p, \lambda)\}$ . This approach is referred to as force-based model updating since entries of residues  $\{Rf(p, \lambda)\}$  in equation (4) are consistent with forces. The alternate approach of enforcing equation (3) is by allowing a

mismatch of vectors that multiply the mass and stiffness matrices

$$[K(p)] \{\psi\} = \lambda [M(p)] \{\phi\} \quad (5)$$

Then, a hybrid residue is defined as the difference between the mode shape  $\{\phi\}$  and the first inverse iterate  $\{\psi\}$  obtained by inverting the stiffness matrix in equation (5). Clearly, the FE model is in good agreement with test data when the “inertia” mode shape  $\{\phi\}$  is equal to the “strain” mode shape  $\{\psi\}$ , resulting in a minimum-norm residue  $\{Rd(p,\lambda)\}$

$$\{Rd(p,\lambda)\} = \{\phi\} - \{\psi\} \quad (6)$$

In theory, these two modal residues are closely related: multiplying equation (6) by the stiffness matrix and substituting equation (5) yields

$$[K(p)] \{Rd(p,\lambda)\} = \{Rf(p,\lambda)\} \quad (7)$$

In practice, implementation constraints (in particular, the spatial incompatibility between measurement and FE discretizations) give rise to a variety of updating and modal expansion techniques for which the condition (7) is not necessarily satisfied. Therefore, a mismatch between the updated models provided by the minimization of residues  $\{Rf(p,\lambda)\}$  and  $\{Rd(p,\lambda)\}$  may be observed, as will be seen in Section 4, even though equation (7) proves that the solution is unique.<sup>3</sup> Note that similar residues may be defined directly with the FRF input-output equation (2), offering a wide range of TAC and FE model updating techniques. Reviews and discussions of state-of-the-art updating methods can be found in Reference [9] for hybrid residues and in References [10-11] for force-based residues.

### 3.2 Discussion of Modal Correlation

Obviously, formulating TAC in the frequency domain offers more advantages than a time-domain approach because: 1) Filtering and averaging are available to alleviate the repeatability issue; 2) Noisy components of the signal and rigid-body modes can be filtered out; and 3) Explicit relationships between test data and FE modeling are available in the form of equations (2-3). For these reasons, model updating procedures for structural dynamics always attempt to

enforce equations (2) or (3) and not the original, time-domain equation of motion (1). Another important justification is that correlating mode shapes is equivalent to matching the subspaces that the measured and simulated responses belong to. This issue is discussed in Section 5.2 when it is attempted to apply the same reasoning to nonlinear test data.

Modal data, however, is only relevant when dealing with linear systems and so confines any correlation done for nonlinear systems to the time domain, forcing us to deal with the problems of multiple field measurement (combinations of displacement, velocity and acceleration data might have to be measured), repeatability and noisy measurements in addition to the already inadequate representation of the system's dynamics.

## 4. LINEAR, MODAL UPDATING OF THE LANL 8-DOF TESTBED

In this Section, we discuss the main results obtained when the linear FE model of the LANL 8-DOF system is updated to match the identified dynamics. As mentioned previously, our testbed exhibits a fair amount of friction which neither the frequency-domain identification algorithm nor the linear FE model account for. Hence, this experiment aims at demonstrating the limitations of inverse modal approaches when the dynamic behavior involved is nonlinear.

Figures 2 and 3 illustrate the updating obtained with the force-based and hybrid formulations, respectively. In this example, the first five identified modes are used, all 8 elements are adjusted and the sensing configuration consists of DOFs 1, 4 and 7 only, although all 8 outputs are available. Note that no measurement is connected to the erroneous spring (attached to masses 5 and 6). This makes it more difficult to find the damage because test mode shapes must be expanded, which undoubtedly introduces additional numerical errors. In Figures 2 and 3, each bar represents the percentage of adjustment brought to the corresponding spring stiffness: an unambiguous damage identification should therefore be limited to a 14% reduction of the fifth stiffness. It can be observed that the two optimal solutions are slightly different: this is due, as mentioned previously, to differences in handling the reconstruction of mode shapes for the non-measured components 2, 3, 5, 6 and 8. The reader is referred to References [8] and [9] for discussions of mode shape expansion associated to force and hybrid residues,

<sup>3</sup> In a finite-dimensional space, all norms are equivalent. Therefore, equation (7) shows that minimizing residues  $\{Rf(p,\lambda)\}$  or  $\{Rd(p,\lambda)\}$  accounts for minimizing the same error using different norms. Thus, convergence patterns may be different but the optimal solution reached upon convergence must be the same in both cases.

respectively. Also, References [12] and [13] present comparative studies of state-of-the-art techniques for solving this critical problem.

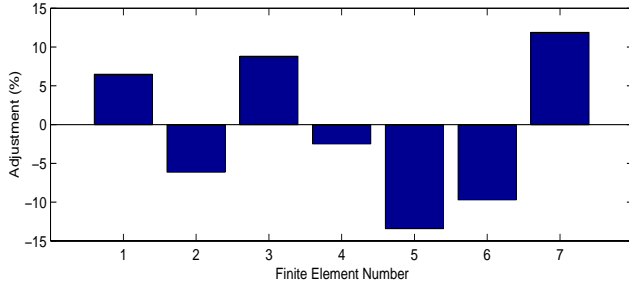


**Figure 2. Adjustments Brought to the Linear FE Model When Force-based Modal Residues Are Minimized.**

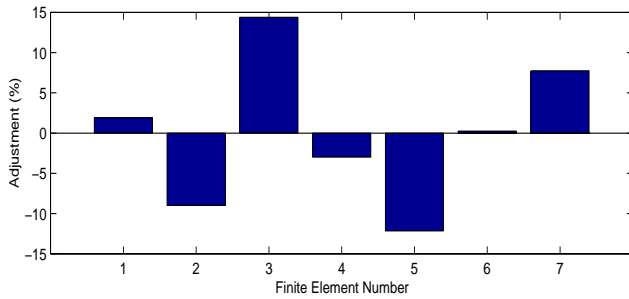


**Figure 3. Adjustments Brought to the Linear FE Model When Hybrid Modal Residues Are Minimized.**

In Figures 2 and 3, both updating techniques identify the correct amount of stiffness reduction at the fifth spring. However, they also bring significant modifications elsewhere in the model: we believe that this is a manifestation of the friction that optimization algorithms attempt to best-fit as stiffness adjustments. Table 3 lists the correlation obtained after force-based optimization. A comparison with Table 2 shows a clear improvement of the predictive quality of our linear model.

**Table 3. TAC After FE Model Updating (Damaged System Vs. Adjusted FE Model).**

Identified Frequency	FE Model Frequency	Frequency Error	MAC
22.3 Hz	22.4 Hz	0.3%	99.9%
43.9 Hz	44.2 Hz	0.6%	99.9%
64.8 Hz	65.9 Hz	1.7%	98.2%
85.9 Hz	85.1 Hz	-0.9%	97.2%
99.7 Hz	99.8 Hz	-0.1%	99.6%

Finally, we have also performed an initial correlation between the FE model and the response of the nominal (undamaged) system. The result is

that the stiffness of the first spring (connected to the driving point measurement) is increased by 22% while all other spring stiffnesses are increased by 5.2% in average. Hence, the initial modeling, too flexible even when no damage is introduced, is improved but this first step does not offset the ambiguous damage identification results obtained when the model is optimized to recover the damaged spring. Using all eight measurement points during the updating provides significantly better results.

We conclude that these results illustrate how modal-based FE updating techniques can be useful tools for improving parametric models. Here, for example, we learn that the driving point attachment produces a local stiffness that should be accounted for in the modeling. At the same time, they show the rapidity with which identification, TAC and updating results deteriorate when the dynamics of interest involve some source or level of nonlinearity.

## 5. TAC FOR NONLINEAR SYSTEMS

We now investigate the formulation of inverse problems for nonlinear structural dynamics. As before, we start with a description of the equation of motion used for the (direct) FE simulations. The correlation metrics are presented in Section 5.1 and it is shown that two different implementations can be proposed for solving basically the same inverse problem.

In this work, nonlinear structural dynamics are described with the following equation of motion

$$[M(p)]\{a(t)\} + [K(p)]\{u(t)\} + \{F_i(p,t)\} = \{F_e(t)\} \quad (8)$$

Equation (8) states that the system is in equilibrium when the applied loading in the right-hand side matches the combination of inertia and internal forces in the left-hand side. The nonlinear internal force vector  $\{F_i(p,t)\}$  accounts for any nonlinear, implicit function of the system's state variables.

Implementing the FE representation (8) is necessary not only because systems we are interested in are nonlinear but also because excitation sources we consider present a lot of high-frequency dynamics. The modal superposition approach becomes ineffective because the loading can not be approximated from the low-frequency modes and because time-domain responses fail to be periodic. Hence, conventional modal analysis does not apply anymore. Numerical models undergo similar

difficulties as computational and accuracy issues arise when extracting high-frequency modes, especially with large dimensional FE models.

### 5.1 TAC & Nonlinear FE Model Updating

In the following, we assume that time-domain, displacement measurements  $\{\mathbf{u}_{\text{test}}(\mathbf{t})\}$  are obtained by instrumenting the system. This assumption is made for simplicity. However, it can be verified easily that all developments below apply to arbitrary combinations of displacement, velocity and acceleration measurements. (Note that higher-order derivatives such as strains could also be employed.)

Since our objective is to generate a refined and more accurate model, the natural TAC metrics to consider are distances between test and simulation data. Residue vectors are defined simply as

$$\{\mathbf{R}(\mathbf{p}, \mathbf{t})\} = \{\mathbf{u}_{\text{test}}(\mathbf{t})\} - \{\mathbf{u}(\mathbf{t})\} \quad (9)$$

The computational procedure consists of the following steps: 1) For a parametric model defined by a design  $\{\mathbf{p}\}$ , the FE response is simulated via numerical integration of equations (8); 2) Residues (9) are calculated at prescribed DOFs and time samples; and 3) The cost function  $\mathbf{J}(\mathbf{p})$  is minimized using an optimization algorithm, where

$$\mathbf{J}(\mathbf{p}) = \|\mathbf{R}(\mathbf{p}, \mathbf{t})\| + \alpha \|\mathbf{p} - \mathbf{p}_0\| \quad (10)$$

It represents the 2-norm (Euclidean norm) of our residue vectors: note that the same definition applies in the linear case with modal residues (4) or (6). It also includes a minimum change term, or regularization term, that helps reducing the numerical ill-conditioning characteristic of inverse problems. From an engineering point-of-view, it simply means that an optimum design  $\{\mathbf{p}\}$  is sought after that brings the least possible change to the original design  $\{\mathbf{p}_0\}$ . The optimization procedure in Step 3 involves multiple FE simulations since time-domain responses must be calculated to evaluate the costs  $\mathbf{J}(\mathbf{p})$  for various designs  $\{\mathbf{p}\}$ . Our current implementation features order-zero algorithms (the simplex method) and order-one algorithms (Gauss-Newton, BFGS and Levenberg-Marquardt, for which documentation can be found in Reference [14]). Gradients are required with order-one optimization methods and they are currently estimated with a centered finite difference scheme, which becomes computationally intensive with large dimensional FE models.

### 5.2 Principal Component Decomposition

The correlation presented previously can be viewed as a rather conventional generalized least-squares (GLS) minimization. The GLS formulation has been used for solving inverse problems in many engineering applications for several decades. It is well known that its success is, to a great extent, conditioned by the ability of the math model to span the subspace to which the test data belongs. It is interesting to notice that this is exactly what modal correlation attempts with linear systems since the measured response belongs to a subspace spanned by the identified mode shapes.

Along these lines, the principal component decomposition (PCD) method developed and validated in Reference [15] attempts to generalize the notion of mode shape for nonlinear systems. Rather than using the direct comparison (9), the SVD of time-domain data is first performed

$$([\mathbf{U}] ; [\mathbf{\Sigma}] ; [\mathbf{V}(\mathbf{t})]) = \text{svd}([\mathbf{u}(\mathbf{t})]) \quad (11)$$

and the residue is basically defined as the distance between test and analysis right-singular vectors

$$\{\mathbf{R}(\mathbf{p}, \mathbf{t})\} = \{\mathbf{V}_{\text{test}}(\mathbf{t})\} - \{\mathbf{V}(\mathbf{t})\} \quad (12)$$

Since the right-singular vectors are orthogonal, they provide a basis of the multi-dimensional manifold to which the nonlinear signals belong [16]. The PCD consists of minimizing the distance between these decompositions rather than between the original signals. Our numerical results presented in Section 6 feature the PCD implementation as it is derived in Reference [15]. (For clarity, the presentation featured in equations (11-12) is a simplified version of the actual method.)

In addition, the SVD offers a practical way of filtering out any measurement noise or rigid-body mode contribution because these are typically associated with singular values much smaller than those characteristic of the dynamics. However, we emphasize that the SVD can **not** be used for detecting if test data are nonlinear. Although attractive, this idea is false: using ingenious initial conditions for integrating the time-response of a simple 4-DOF mass-spring system (see Section 6.1), the PCD can be “fooled” and lead to believe that the response is nonlinear (because, often, the shapes of right-singular vectors  $\{\mathbf{V}(\mathbf{t})\}$  are characteristic of

whether or not the system is nonlinear) when it is, in fact, perfectly linear.

## 6. NONLINEAR UPDATING OF THE LANL 8-DOF TESTBED

In this Section, we present an overview of the results that have been obtained with the time-domain FE model correlation and updating procedure. In Section 6.1, a validation based on data simulated numerically is discussed. In Section 6.2, the LANL 8-DOF testbed is analyzed in an attempt to identify the nonlinear contact/impact force.

### 6.1 Validation Using Simulation Results

The validation presented here employs the 4-DOF mass-spring system depicted in Figure 4 where the fourth spring exhibits a cubic stiffness. The “test” data are simulated numerically and feature a 15% stiffness reduction of the (linear) third spring combined to a 25% stiffness increase of the (nonlinear) fourth spring. Simulations run up to 0.2 seconds and the response is sampled at 200 equally-spaced points in the [0;0.2] sec. interval and at DOFs 1, 3 and 4. The second DOF is not measured which leaves us the choice to either condense the FE matrices down to the subset of measurement points available or to work with full-order matrices. No external force is applied to the system; instead, the first mode shape of the associated linear model is used as initial condition for initializing the time integration. We emphasize that this system is nonlinear since it results from the combination of a linear model (where all four spring stiffnesses are linear) and a nonlinear internal force applied to the fourth mass and proportional to the third power of the fourth displacement.

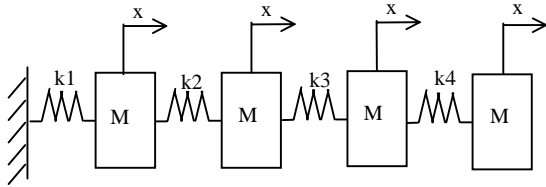


**Figure 4. 4-DOF Nonlinear System.**

During the correlation, the distance between “measured” and simulated displacements at DOFs 1, 3 and 4 is minimized. Figures 5 and 6 illustrate a typical comparison of displacement responses before and after model updating, respectively. Clearly, the FE responses (shown in dashed line) match more closely the “test” data (shown in solid line) after the optimization. Table 4 compares the updating results obtained with four different implementations of our

time-domain TAC technique. For each method, the first four rows list the percentages of stiffness adjustment brought to the linear springs. The fifth row lists the percentages of adjustment brought to the cubic spring stiffness. The correct answer is therefore -15% in row, and +25% in row 5 and no adjustment elsewhere in the model.

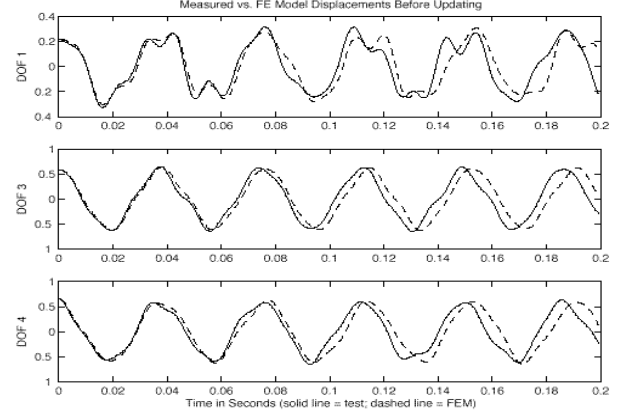


**Figure 5. Displacement Time History Before Updating the 4-DOF Nonlinear Model.**

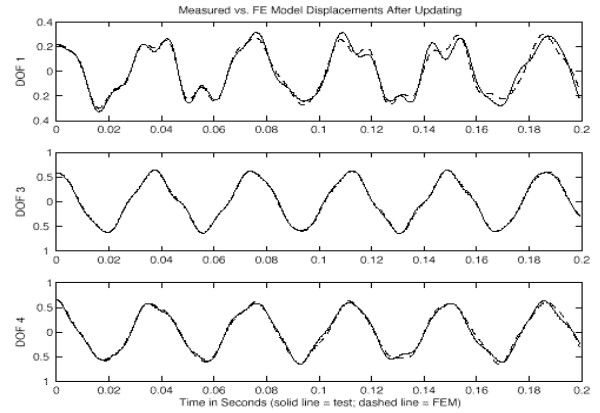


**Figure 6. Displacement Time History After Updating the 4-DOF Nonlinear Model.**

In Table 4, results of the GLS approach with FE model reduction (MR) are presented in columns 1 and 2; in the second column, both displacement and velocity data are used for updating the model. When displacements only are inputted to the minimization, the solution expected is not reached. Nonetheless, the adjustment featured in column 1 reproduces almost exactly the displacement “test” data, which reminds us of the non-unicity of the solution. To resolve this difficulty, velocity data are added and the optimization then converges to the expected solution (see column 2). Results of the PCD approach using full-order matrices (FM) and model reduction are presented in columns 3 and 4, respectively. Both

simulations are based on displacement data only and both provide excellent results. Comparing columns 3 and 4 shows that the solution is slightly deteriorated when MR is used. Condensing the FE matrices may be necessary for initializing correctly the time integration procedure and should moreover lead to significant CPU time reductions with large FE models.

**Table 4. Optimized 4-DOF FE Models Obtained With Various Implementations.<sup>4</sup>**

GLS, MR D-data	GLS, MR D, V-data	PCD, FM D-data	PCD, MR D-data
6.4%	0.1%	0.2%	1.6%
4.3%	0.5%	1.4%	5.9%
-1.7%	-14.9%	-13.5%	-12.1%
-3.0%	-0.3%	-1.0%	-3.8%
5.9%	24.6%	22.1%	20.8%

There is no noticeable advantage of one approach over the others in regard to computational cost, which is not surprising considering the small size of this system. It is noticed, however, that order-one optimization algorithms require much fewer iterations to reach convergence, the drawback being a high computational requirement (per iteration) for estimating the cost function's gradients.

## 6.2 Application to the LANL 8-DOF Testbed

In this Section, model updating is applied to the LANL 8-DOF testbed. The objective is to correlate transient, time-domain test data obtained by instrumenting the system's nonlinear configuration. Here, the contact mechanism is enabled during modal tests. Figure 7 illustrates the small clearance between the fifth and sixth masses. Therefore, a source of contact/impact is introduced during vibrations.



**Figure 7. Contact Mechanism of the LANL 8-DOF Testbed.**

<sup>4</sup> Symbols used in Table 4 are: GLS, generalized least-squares; PCD, principal component decomposition; MR, model reduction; FM, full-order model (no reduction); D-data, displacement data; and V-data, velocity data.

Random, input excitations at the driving point (DOF 1) and the eight accelerations are measured at 4,096 samples over a time period of 8 seconds. Data are collected for various force levels to identify the degree of nonlinearity.

Although all DOFs are measured during vibration tests, we assume that data are available at DOFs 1, 5 and 6 only. Therefore, the correlation consists of matching these three acceleration time-histories with results from the numerical simulation. Since the correlation involves three DOFs only, model reduction is implemented to condense the FE matrices and force vectors. The particular technique chosen preserves exactly the lowest frequencies and mode shapes of the linear model [17]. Figure 8 illustrates the correlation before FE model updating.

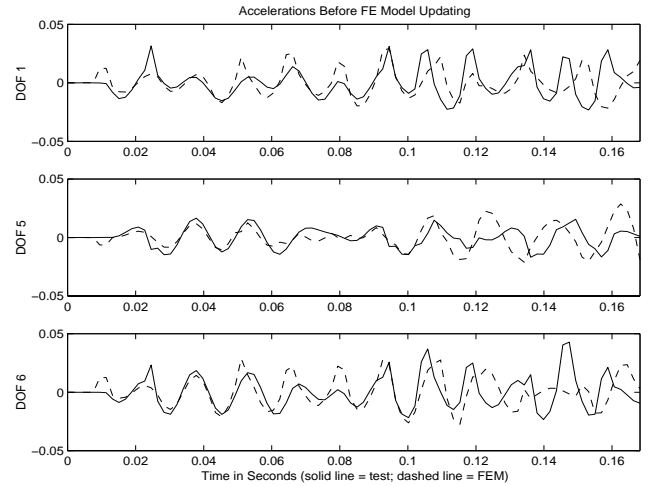


**Figure 8. Acceleration Time History Before Updating the LANL 8-DOF Testbed.**

As in Section 4, our modeling of this system is perfectly linear, except for the addition of an internal force vector. First, we attempt to represent the nonlinearity as an internal force triggered when contact or penetration are detected during time integration. Forces applied to masses 5 and 6 are opposite in direction (such that the two masses are pushed away from each other) and proportional to the depth of penetration. Therefore, this simple contact model is parametrized by the amount of penetration allowed and the stiffness of the reaction force. However, attempts to update these parameters have proven unsuccessful so far.

A second approach is pursued using a non-parametric force vector. Arbitrary internal forces are applied at each one of the eight masses of the system and TAC is used for estimating these force levels at prescribed time samples.

The overall procedure goes as follows. Unknowns of the optimization are the eight force components. Correlation is based on the first 90 acceleration measurements that span the time window [0;0.168] sec. For the numerical simulation, FE matrices and force vectors are reduced to the size of the TAC model (DOFs 1, 5 and 6 only) and the response of the condensed model is integrated in time using 10 sampling points between any two measurements. As the FE response is integrated in time, the internal force vector is optimized.

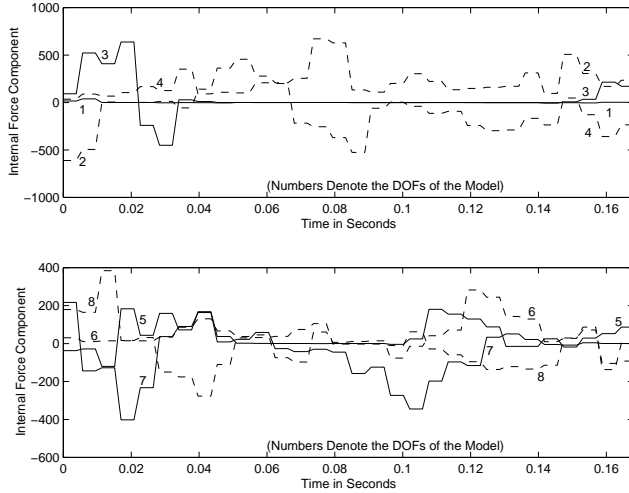


**Figure 9. Time-Histories of Internal Forces Obtained Via FE Model Correlation.**

Figure 9 shows the reconstruction of internal force as optimizations are performed for each time interval containing three consecutive measurements. In other words, 30 optimizations are performed, one every 0.0056 sec. This result is obtained when the GLS cost function is optimized (no SVD is involved here). Obviously, no clear interpretation of this forcing function can be made. Notice however that the internal force at DOF 1 is approximately equal to zero. It seems consistent with the fact that DOF 1 is the driving point where random excitation is applied.

It can be observed that, to the exception of DOF 1 where the external force is applied, all DOFs feature significant levels of internal force even though they are not directly involved with the nonlinear mechanism. This might be a manifestation of the system's friction. However, these results are preliminary and further investigation is required before any plausible assessment of these forces can be made. No matter what the source of the internal force turns out to be, Figure 10 shows a clear improvement of the correlation with test data when this force vector is included in the FE simulation.

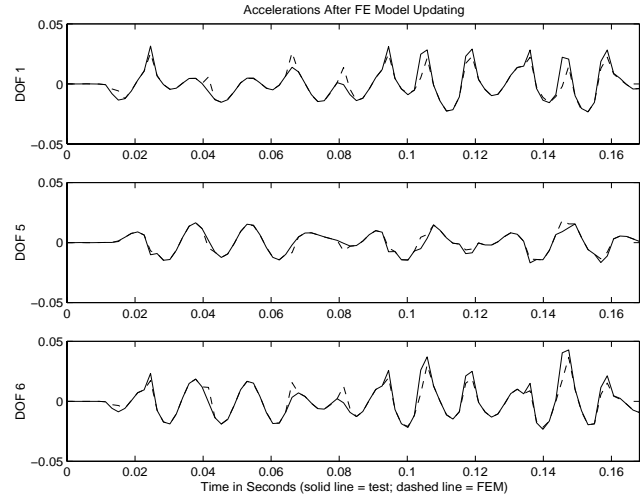


**Figure 10. Acceleration Time History After Updating the LANL 8-DOF Testbed.**

We emphasize that results presented here constitute a first step: non-parametric model updating does not necessarily yield a sound understanding of the system's physics. For all practical purposes, a second identification would be required to generate a useful, parametrized nonlinear model.

## 7. CONCLUSION

This work presents an investigation of the correlation of test data to finite element models for nonlinear, transient dynamics. Modal techniques in the frequency domain are discussed and it is shown that they fail to correlate a linear model when the experimental data involves significant friction. Therefore, the correlation is formulated in the time domain and the merits of two implementations are compared using test data from the LANL 8-DOF nonlinear testbed.

The preliminary results obtained are very encouraging and additional full-scale testing is planned with these and other methods. In particular, the optimal control-based formulation proposed in Reference [18] seems very promising because it enables the non-parametric identification of unmodeled nonlinear dynamics. It is currently being interfaced with our modeling and correlation software.

## ACKNOWLEDGMENTS

The authors would like to recognize the contribution of Paula Beardsley, Graduate student at the University of Washington, Seattle, Washington,

who produced some of the results presented in this paper during a Summer 1998 internship at LANL. Data acquisition was performed at LANL by Bill Baker, Tom Duffey, Technical Staff Members, and Winston Rhee, Graduate student from Texas Tech University. Also, the expertise and guidance of Dr. Thomas D. Burton, Chairman of the Department of Mechanical Engineering at Texas Tech University, Lubbock, Texas, is acknowledged and gratefully appreciated.

## REFERENCES

- [1] Lieven, N.A.J., and Ewins, D.J., "A Proposal For Standard Notation and Terminology in Modal Analysis," *10th IMAC*, Feb. 2-5, 1992, San Diego, California, pp. 1414-1419.
- [2] Masri, S.F., Miller, R.K., Saud, A.F., and Caughey, T.K., "Identification of Nonlinear Vibrating Structures: Part I - Formulation," *ASME Journal of Applied Mechanics*, Vol. 54, Dec. 1987, pp. 918-922.
- [3] Zienkiewicz, O.C., and Taylor, R.L., **The Finite Element Method**, 4th Edition, McGraw-Hill, London, U.K., 1989.
- [4] Maia, N.M.M., and Silva, J.M.M., **Theoretical and Experimental Modal Analysis**, Ed., Research Studies Press, Ltd., Wiley & Sons, New York, 1997.
- [5] Alvin, K.F., Peterson, L.D., and Park, K.C., "Extraction of Normal Modes and Full Modal Damping From Complex Modal Parameters," *AIAA Journal*, Vol. 35, No. 7, July 1997, pp. 1187-1184.
- [6] Berman, A., and Nagy, E.J., "Improvement of a Large Analytical Model Using Test Data," *AIAA Journal*, Vol. 21, No. 8, Aug. 1983, pp. 1168-1173.
- [7] Imregun, M., and Visser, W.J., "A Review of Model Updating Techniques," *Shock and Vibration Digest*, Vol. 23, No. 1, 1991, pp. 19-20.
- [8] Farhat, C., and Hemez, F.M., "Updating Finite Element Dynamic Models Using an Element by Element Sensitivity Methodology," *AIAA Journal*, Vol. 31, No. 9, Sept. 1993, pp. 1702-1711.
- [9] Chouaki, A.T., Ladevèze, P., and Proslie, L., "Updating Structural Dynamics Models With Emphasis on the Damping Properties," *AIAA Journal*, Vol. 36, No. 6, June 1998, pp. 1094-1099.
- [10] Hemez, F.M., "Can Model Updating Tell the Truth?," *16th IMAC*, Santa Barbara, California, Feb. 2-5, 1998, pp. 1-7.
- [11] Mottershead, J.E., and Friswell, M.I., "Model Updating in Structural Dynamics: A Survey," *Journal of Sound and Vibration*, Vol. 162, No. 2, 1993, pp. 347-375.
- [12] Hemez, F.M., "Comparing Mode Shape Expansion Methods For Test-Analysis Correlation," *12th IMAC*, Jan. 31-Feb. 3, 1994, Honolulu, Hawaii, pp. 1560-1567.
- [13] Levine-West, M., Kissil, A., and Milman, M., "Evaluation of Mode Shape Expansion Techniques on the Micro-Precision Interferometer Truss," *12th IMAC*, Jan. 31-Feb. 3, 1994, Honolulu, Hawaii, pp. 212-218.
- [14] Jacobs, D.A.H., **The State of the Art in Numerical Analysis**, Ed., Academic Press, London, U.K., 1977.
- [15] Hasselman, T.K., Anderson, M.C., and Wenshui, G., "Principal Components Analysis For Nonlinear Model Correlation, Updating and Uncertainty Evaluation," *16th IMAC*, Santa Barbara, California, Feb. 2-5, 1998, pp. 664-651.
- [16] Mees, A.I., Rapp, P.E., and Jennings, L.S., "Singular Value Decomposition and Embedding Dimension," *Physical Review A*, Vol. 36, No. 1, July 1987, pp. 340-346.
- [17] Burton, T.D., and Young, M.E., "Model Reduction and Nonlinear Normal Modes in Structural Mechanics," *ASME AMD*, Vol. 192, 1994, pp. 9-16.
- [18] Dippery, K.D., and Smith, S.W., "An Optimal Control Approach to Nonlinear System Identification," *16th IMAC*, Santa Barbara, California, Feb. 2-5, 1998, pp. 637-643.